An Intelligent ANFIS-Based Control System for Upper-limb Exoskeleton Robot

Shao-Fu Jiang, Hsin-Chieh Chien, Po-Hsiang Lin, Kuu-Young Young, and Chun-Hsu Ko

***Abstract*—As the aging population continues to grow, the exoskeleton robots are developed for assistance of rehabilitation and daily activities for the elderly. In this paper, we propose an assistive motion control system based on user intention for the upper-limb exoskeleton robot. The system detects user intention through electromyography (EMG) signal analysis first, and then utilizes an adaptive neural fuzzy inference system (ANFIS) to estimate proper torque to assist user's motion. The experimental results show that the proposed system allows the users to manipulate the exoskeleton robot according to their intention with lesser effort, thus demonstrating its effectiveness.**

***Index Terms*—Upper-limb exoskeleton robot, Motion assistance, ANFIS, EMG**

I. Introduction

ALONG with the advent of the aging society, elderly care has become an increasingly important issue. Elder people may experience upper-limb weakness or difficulty with limb movement to conditions such as stroke, leading to a need for movement support. As exoskeleton robots [1]-[6] can provide motion assistance for tasks related to upper limbs, it is much helpful for their development to provide daily assistance and rehabilitation for the elderly and individuals with limited mobility.

Among previous research on upper limb exoskeleton robots, Krebs et al. [1] proposed the MANUS system to guide the movement of a user's upper limb during rehabilitation. Kooren et al. [2] designed a 5-degree-of-freedom upper limb exoskeleton robot to assist individuals with muscle weakness. Chen et al. [3] developed a 7-degree-of-freedom upper limb exoskeleton robot system that effectively facilitates upper limb rehabilitation. Cui et al. [4] developed a cable-driven arm exoskeleton for dexterous motion training and assistance. Zeiaee et al. [5] designed a lightweight and compact exoskeleton for upper-limb rehabilitation. Garzo et al. [6] proposed a telerehabilitation platform designed to help users maintain upper-limb rehabilitation at home. Via the survey, the exoskeleton robots are in general operated in two modes: passive and active [7]. The passive mode allows the robot to govern limb movement by itself, and the user does not need to exert any effort for task execution. In contrast, the active mode enables the robot to provide assistive torque to aid the movement, while users actively move their limbs according to their intention. It is thus very crucial on accurate detection of user's intention for providing proper assistive torque.

Electromyography (EMG) [8]-[12], electroencephalography (EEG) [13], and force information [14] are commonly adopted by the exoskeleton robot to detect user's intention. EMG signals are measured from muscle activity to reflect user's intention via analysis. Lotti et al. [8] introduced a myoprocessor model capable of predicting muscle forces based on EMG and arm movement data. Lenzi et al. [9] used proportional EMG control in a powered exoskeleton to assist the user's elbow movement. Furukawa et al. [10] estimated the intended movements by observing EMG signals with uncertain observations taken into account. Koike et al. [11] estimated user's joint torque from EMG using a neural network. Kiguchi et al. [12] developed a joint torque model based on EMG and applied a neuro-fuzzy modifier to adapt the model for different users. Because EMG signals are often motion-related and highly nonlinear, effective EMG-based intention detection and control remains in demand.

In this paper, we propose an effective assistive control system based on the EMG to govern a two-DOF upper-limb exoskeleton robot by employing the Adaptive Neuro-Fuzzy Inference System (ANFIS) [15]. Compared to previous approaches, it has the advantage of combining interpretability through fuzzy if-then rules with parameter optimization via neural network learning, so that system uncertainty and non-linearity of the system can be well tackled. During task execution, the EMG signals are first measured and analyzed, and then sent for a torque model developed based on the ANFIS to estimate the assistive torque, which is further processed by the designed controller to generate robot motion commands. Finally, experiments based on applying the proposed system for upper-limb motion assistance are conducted for performance evaluation.

The remainder of this paper is organized as follows: Section II describes the mechanism and dynamics of the upper-limb exoskeleton robot. In Section III, the proposed system is addressed. Experimental results are presented in Section IV. Finally, concluding remarks are given in Section V.

II. Upper-limb Exoskeleton Robot

The developed two-DOF upper-limb exoskeleton robot [16] is as shown in Fig. 1. The robot is fixed on a base to provide assistive torques to support the user's upper-limb movement. Its design includes forearm and upper arm links, fixed base, elbow and shoulder joint motors, the encoders, and a controller. The shoulder joint is a single-axis mechanism that allows the arm to move vertically, with the motor providing the joint torque to assist in raising and lowering the arm. The elbow

This work was supported in part by the Ministry of Science and Technology, Taiwan under grant MOST 110-2221-E -214-024.

Chun-Hsu Ko and Hsin-Chieh Chien are with the Department of Electrical Engineering, I-Shou University, Kaohsiung, Taiwan (corresponding author: Chun-Hsu Ko, e-mail: chko@isu.edu.tw).

Shao-Fu Jiang and Kuu-Young Young are with the Department of Electrical Engineering, National Yang Ming Chiao Tung University, Hsinchu, Taiwan.

Po-Hsiang Lin is with the Department of Emergency Medicine, Kaohsiung Veterans General Hospital, Kaohsiung, Taiwan.

Manuscript received 19 December 2024; revised 16 March 2025; accepted 5 April; Date of publication 30 April 2025.

Fig. 1. The photo of the developed upper-limb exoskeleton robot.

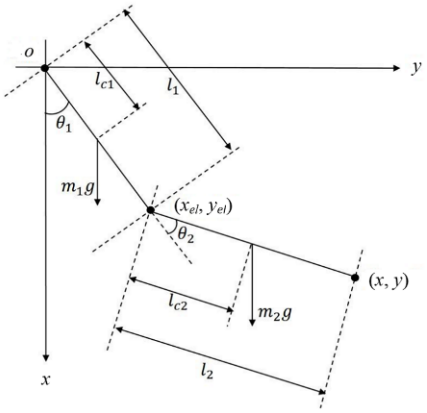

Fig. 2. Configuration of the upper-limb exoskeleton robot.

joint is also a single-axis mechanism, with the motor providing torque to assist the extension and flexion of the upper arm and forearm. The encoders measure joint rotation angles, and the controller computes the necessary assistive torques. To ensure consistency between the upper-limb exoskeleton and the human arm, the position and length of the links can be adjusted according to user's demand.

The configuration of the upper-limb exoskeleton robot is as shown in Fig. 2, which illustrates a biaxial model of the shoulder and elbow joints. The origin o is the position of the shoulder joint, (x_{el}, y_{el}) that of the elbow joint, and (x, y) the end point position of the robot. The x-axis represents the direction of the arm when it is vertically lowered, and the y-axis that of the arm when raised horizontally. m_1 and m_2, I_1 and I_2, and l_1 and l_2 are the masses, moments, and lengths of the upper arm and forearm, respectively, l_{c1} and l_{c2} the distances between the centers of mass of the upper arm and forearm and the axis position, respectively, and g the gravity.

The joint angle θ of the exoskeleton robot is given by

$$\theta = \begin{bmatrix} \theta_1 & \theta_2 \end{bmatrix}^T \tag{1}$$

where θ_1 is the raising angle of the upper arm relative to x-axis, and θ_2 that of the forearm relative to the upper arm. With the torque

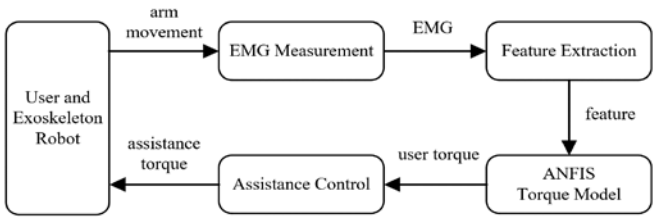

Fig. 3. The proposed motion control system.

$$\tau = \begin{bmatrix} \tau_1 & \tau_2 \end{bmatrix}^T \tag{2}$$

where τ_1 and τ_2 are the shoulder and elbow joint torque, respectively, the dynamic equation of the upper-limb exoskeleton robot is derived as

$$M(\theta)\ddot{\theta} + V(\dot{\theta}, \theta) + G(\theta) = \tau \tag{3}$$

with

$$M = \begin{bmatrix} m_1 l_{c1}^2 + I_1 + m_2(l_1^2 + l_{c2}^2 + 2l_1 l_{c2}\cos\theta_2) + I_2 & m_2(l_{c2}^2 + l_1 l_{c2}\cos\theta_2) + I_2 \\ m_2(l_{c2}^2 + l_1 l_{c2}\cos\theta_2) + I_2 & m_2 l_{c2}^2 + I_2 \end{bmatrix}$$

$$V = \begin{bmatrix} -m_2 l_1 l_{c2}\left(2\dot{\theta}_1\dot{\theta}_2 + \dot{\theta}_2^2\right)\sin\theta_2 \\ m_2 l_1 l_{c2}\dot{\theta}_1^2 \sin\theta_2 \end{bmatrix} \tag{4}$$

$$G = \begin{bmatrix} (m_1 l_{c1} + m_2 l_1) g \sin\theta_1 + m_2 l_{c2} g \sin(\theta_1 + \theta_2) \\ m_2 l_{c2} g \sin(\theta_1 + \theta_2) \end{bmatrix}$$

where M is the inertia matrix, V the centripetal Coriolis and viscosity, and G the gravity term.

With the user conducting arm movement under robot assistance, the dynamic equation can be expressed as

$$M(\theta)\ddot{\theta} + V(\dot{\theta}, \theta) + G(\theta) = \tau_h + \tau_r \tag{5}$$

where τ_h and τ_r are the torques applied by the user and robot, respectively. With the dynamic equation of the upper limb exoskeleton robot available, the proposed assistance control system is derived as follows.

III. Proposed Control System

The proposed control system is as shown in Fig. 3. The user wears the exoskeleton robot for upper limb movement. The EMG measurement device detects EMG signals generated by muscle activity. The signals are then processed through EMG feature analysis to extract relevant features. Using these features along with the robot's biaxial angles, the ANFIS torque model estimates user's torque. Consequently, the assistance controller derives the necessary torque to drive the exoskeleton robot to support limb movement. The procedure will be repeated until the task is completed. The realization of EMG feature extraction, torque model building, and assistance control are described as follows.

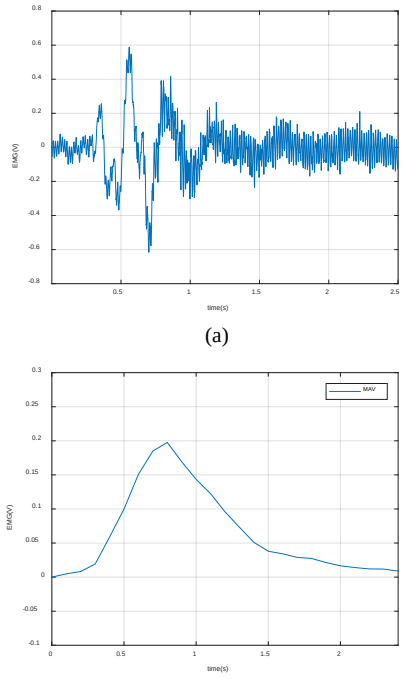

(a)

(b)

Fig. 4. Biceps EMG signals: (a) measured signal and (b) MAV.

A. *EMG Feature Extraction*

First, the electrode patches placed on the surface of the skin are utilized to measure the EMG signals from arm muscles. For the shoulder joint, the anterior and posterior deltoid muscles are responsible for the lifting and lowering actions, respectively. The biceps brachii muscle is primarily responsible for elbow flexion, while that of the triceps brachii facilitates elbow straightening. As the arm muscles are activated, the measurement equipment detects time-varying EMG signals, which are then processed using a band-pass filter between 3 Hz and 2 kHz to reduce noise and improve signal quality.

Since the frequency band of the detected EMG signals ranges from 10 to 500 Hz, a fourth-order Butterworth band-pass filter with a range of 40 to 400 Hz was applied to remove interference noise. To obtain the relationship between signal amplitude and muscle activation, a full-wave rectifier was adopted, which converted the oscillating EMG signals into positive amplitudes by taking their absolute values. The Kalman filter was applied to further reduce noise. Finally, by computing the mean absolute value (MAV) [17], the EMG feature can then be obtained:

$$\mathrm{MAV} = \frac{1}{n_s}\sum_{i=1}^{n_s}\left|x_i\right| \tag{6}$$

where n_s is the total number of EMG signal samples, and x_i represents the amplitude of the i-th sample.

For verification of the proposed method, we measured the biceps EMG signal by moving the elbow upward by a certain distance, as shown in Fig. 4(a), with the corresponding MAV shown in Fig. 4(b). It can be observed that the noise in the measured biceps EMG has been properly filtered through the signal processing procedure, and the resulting smooth MAV signal effectively reflects the muscle activity. We therefore apply it to derive the corresponding MAV from the anterior deltoid, posterior deltoid, biceps brachii, and triceps brachii muscles during arm movements for exoskeleton robot governing.

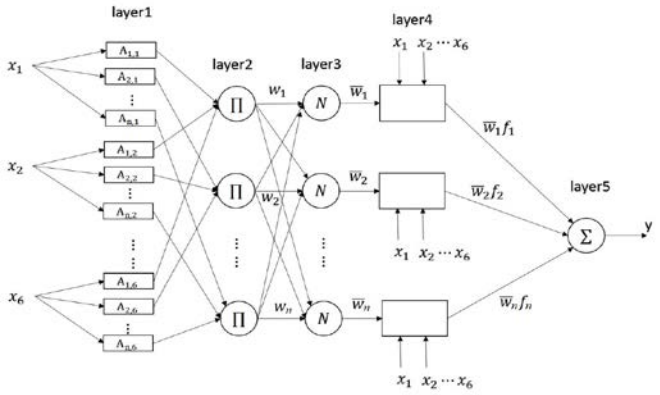

Fig. 5. The ANFIS structure.

B. *ANFIS Torque Model Building*

To determine the torque applied during user's upper-limb movements, the torque models based on ANFIS are built for the shoulder and elbow joints. The inputs are the EMG features derived from arm muscle activities, along with the biaxial angles of the exoskeleton robot, and the output is the corresponding torque. Because the relationship between input and output is nonlinear, we employed ANFIS [15] for model building. ANFIS integrates adaptive learning with interpretable modeling, enabling it to effectively model complex systems, which well serves our purpose. Its structure is as shown in Fig. 5, which consists of five layers:

Layer 1: The layer determines the membership degree of the input in the fuzzy set using the Gaussian membership function:

$$\mu_{A_{ij}}(x_j) = \exp[-\frac{1}{2}(\frac{x_j - c_{ij}}{\sigma_{ij}})^2], i = 1,\cdots,n,\ j = 1,\cdots,6 \tag{7}$$

Layer 2: The firing strengths of the fuzzy rules are calculated using product operations:

$$w_i = \mu_{A_{i1}}(x)\times\mu_{A_{i2}}(x)\cdots\times\mu_{A_{i6}}(x), i = 1,\cdots,n \tag{8}$$

Layer 3: This layer normalizes the firing strengths of the rules:

$$\overline{w}_i = \frac{w_i}{\sum_{j=1}^{n} w_j} \tag{9}$$

Layer 4: This layer performs the inference operations for each fuzzy rule:

$$f_i(x) = p_{i0} + p_{i1}x_1 + p_{i2}x_2 + \cdots + p_{i6}x_6 \tag{10}$$

where p_{i0}, p_{i1}, …, p_{i6} are the parameters of the inference part.

Layer 5: The results of the fourth layer are summed to produce the output:

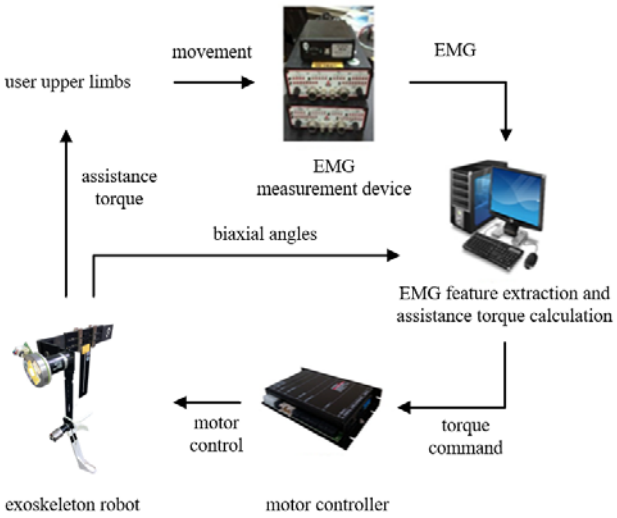

Fig. 6. The experimental setup.

Fig. 7. The experimental scene.

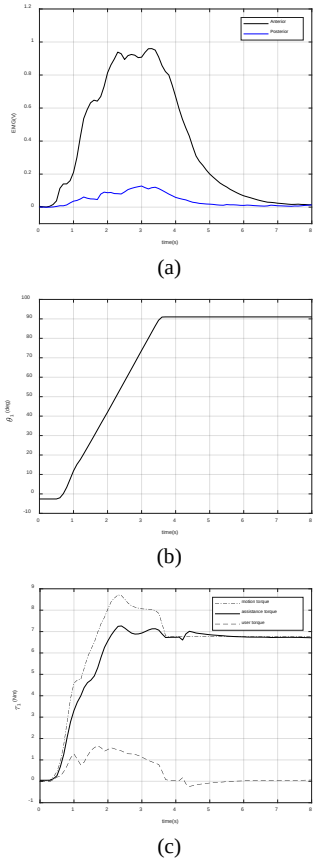

(a) (b) (c)

Fig. 8. Experiment results for shoulder-lifting motion: (a) shoulder EMG signal, (b) shoulder angle, and (c) shoulder torques.

$$y = \sum_{i=1}^{n} \overline{w}_i f_i \tag{11}$$

Training data was collected with the users conducting single-axis movements of the elbow and shoulder, as well as dual-axis ones involving both joints simultaneously, which were commonly associated with upper-limb motions in daily activities. It was not obtained by measurement, but calculated based on the robot's dynamic model and detected joint trajectory. As the goal of the training is to let the exoskeleton robot provide gravity compensation and suitable torques to assist the user during motions, the data recorded includes EMG features, biaxial angles, and assistive torques. Among these, the EMG features and biaxial angles serve as inputs to the torque model, and the output is the user's torque τ_h, which can be calculated as

$$\tau_h = M(\theta)\ddot{\theta} + V(\dot{\theta},\theta) + G(\theta) - \tau_{rt} \tag{12}$$

where τ_{rt} is the torque exerted by the robot for training data collection. To obtain the parameters for the model, the Fuzzy C-Means clustering algorithm is first applied to divide the training data into groups. Fuzzy rules and their initial parameters are then generated based on the data from each group. The ANFIS training method [15] is used to learn and adjust the parameters of the antecedent and inference parts of the fuzzy rules based on input and output training data.

C. Assistance Control

The assistance controller should provide certain assistive torque, so that the user may exert less effort during task execution. It can be regarded as that the user and robot jointly share the forces necessary for the movement. Therefore, the user may feel experiencing a lighter robot system, with the dynamic equation [18] expressed as

$$M_d\ddot{\theta} + V_d + G_d = \tau_h \tag{13}$$

where M_d, V_d, and G_d are calculated from Eq. (4) using the reduced mass of the system that the user experiences. From Eq. (5) and Eq. (13), the robot assistive torque τ_r can be expressed as

$$\tau_r = (M - M_d)\ddot{\theta} + (V - V_d) + (G - G_d) \tag{14}$$

From Eq. (13), the angular acceleration can be obtained as

$$\ddot{\theta} = M_d^{-1}(\tau_h - V_d - G_d) \tag{15}$$

Substituting Eq. (15) into Eq. (14), τ_r can be calculated as

$$\tau_r = (M - M_d)M_d^{-1}(\tau_h - V_d - G_d) + V - V_d + G - G_d \tag{16}$$

With the above control law, the robot's control torque can be determined using the user's applied torque estimated

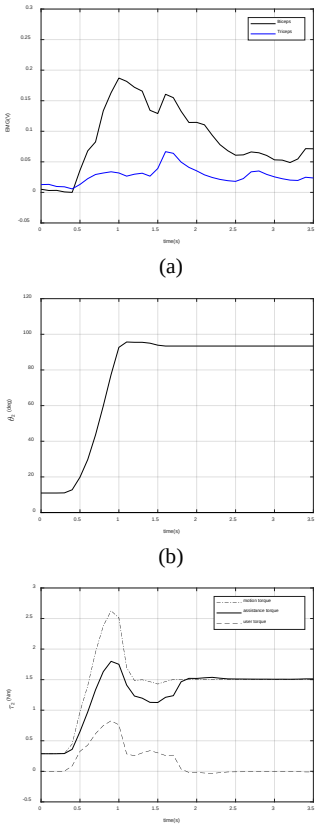

(a)

(b)

(c)

Fig. 9. Experimental results for elbow-bending motion: (a) elbow EMG signal (b) elbow angle, and (c) elbow torques.

by the ANFIS model.

Note that, because the measured EMG signals may contain noise, to avoid abrupt change of τ_r, we came up with a procedure via checking the statuses of both the current and previous EMG signals. When they implicate the opposite movement direction, the newly derived τ_r will be adopted only when it occurred twice, otherwise, previous τ_r was maintained. As for the case with the same implication, the derived τ_r is used directly. By applying this procedure, the assistive torque will not vary significantly, leading to stable movement.

IV. Experiments

We conducted a series of experiments to verify the effectiveness of the proposed system. The experimental setup is illustrated in Fig. 6. When the user moves their upper limbs, EMG signals are detected using the electrode patches (Kendall Medi-Trace) and amplified by a biopotential preamplifier (C-ISO-255) and a biopotential amplifier (iWorx ETH-256). These signals are then forwarded to the computer via the data recorder (IX-404) for filtering and feature extraction. The torque model estimates user's applied torque based on EMG features and detected biaxial angles. The assistance controller in turn computes the desired assistive torque and convert it into a motion command sent to the motor controller to move the exoskeleton robot. The experimental scene is as shown in Fig. 7, in which the subject wore an upper-limb exoskeleton robot to conduct tasks involving one- or two-joint motions. Five subjects, aged between 22 to 24, were invited to participate.

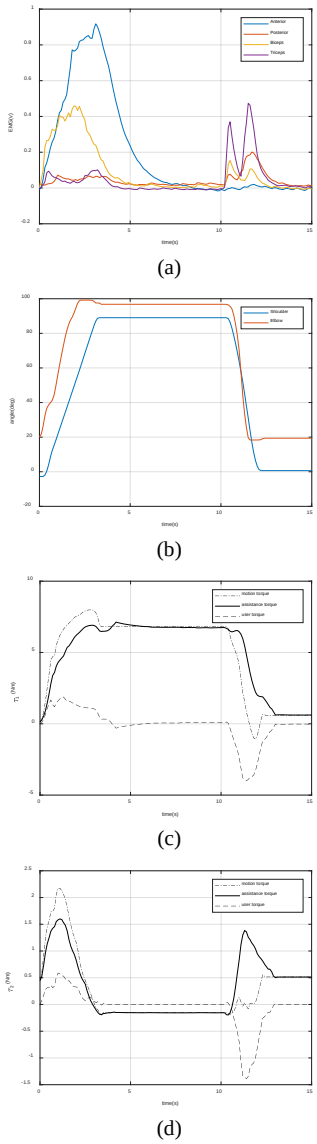

(a)

(b)

(c)

(d)

Fig. 10. Experimental results for two-joint motion: (a) EMG signals, (b) arm angles, (c) shoulder torques, and (d) elbow torques.

Before the experiment, training data were collected from each subject for building the corresponding torque model in advance.

The first set of experiments were intended for one-joint motion, including shoulder lifting and lowering and also elbow bending and straightening. Fig. 8 shows the experimental results for the shoulder joint for one of the subjects, including the EMG signals, arm angles, and shoulder torques, which were typical among others. It was observed that the EMG signal of anterior deltoid increased and then decreased as the shoulder angle increased, which well implicated user's intention for shoulder lifting. Meanwhile, in addition to gravity compensation, the assistive torque did provide support for shoulder lifting, thus reducing user's load by letting the applied torque smaller than the required one. Fig. 9 shows the results for the elbow joint. Similar phenomena were observed, including variations of the biceps EMG signals, elbow angle, and elbow torques. We continued conducting experiments for shoulder lowering and elbow straightening. It was found that variations of EMG signals for the posterior

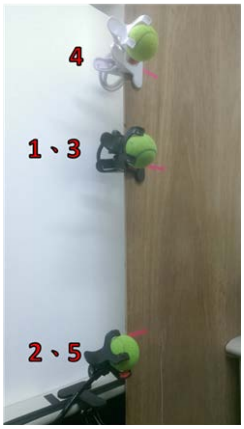

Fig. 11. The target positions for the ball-touching experiments.

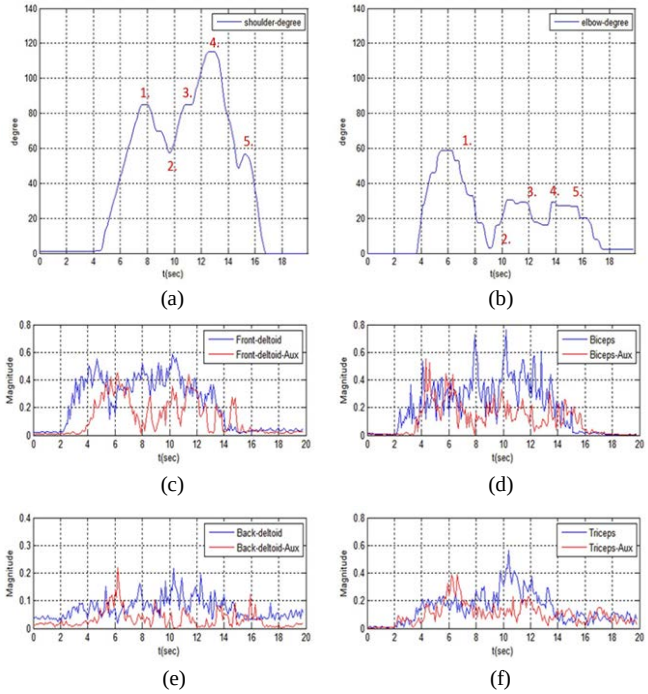

Fig. 12. Experimental results for ball-touching motion: (a) shoulder angle, (b) elbow angle, (c) front-deltoid EMG signals with and without assistance, and (d) biceps EMG signals with and without assistance (e) back-deltoid EMG signals with and without assistance, and (f) triceps EMG signals with and without assistance.

deltoid and triceps aligned with that of the angles during shoulder lowering and elbow extension. These results demonstrated that the proposed system has effectively detected user's intention and yielded appropriate assistive torque for single-joint motion.

The second set of experiments were intended to evaluate whether the proposed system was capable for handling two-joint motions, which involves coupling between the joints. During the experiments, the subject raised both the shoulder and elbow up to approximately 90 degrees and then lowered them back to the original position. Fig. 10 shows the experimental results, including the EMG signals, arm angles, and shoulder and elbow torques. When the arm was raised, the EMG signals of the anterior deltoid and biceps increased and then decreased; while it was lowered, that of the posterior deltoid and triceps increased and then decreased. With user's intention well predicted and the effect of the torque model, appropriate assistive torques for both joints were provided, leading to its successful execution, even in the presence of coupling.

Finally, in the third set of experiments, we asked the subject to conduct a ball-touching task with and without wearing the exoskeleton robot, which were intended to evaluate system performance for a reaching action that commonly occurred in our daily activity. As shown in Fig. 11, the subject needed to touch the balls following a given order. He/she should pause briefly upon touch. Fig. 12 shows one typical result, including the angles for both the shoulder and elbow, and their corresponding EMG signals with and without assistance. No matter with or without wearing the exoskeleton robot, all the subjects completed the task successfully, while less effort was demanded when it was with assistance, as implicated by smaller EMG signals present in Figs. 12(c)–(f).

V. Conclusion

In this paper, we have developed an intelligent control system based on ANFIS for the upper-limb exoskeleton robot, which can be used to assist the user for motions in daily activities. The EMG signals measured during user's movement was analyzed to estimate his/her motion intention, and then sent for the ANFIS toque model and assistance controller to generate the corresponding motion commands. Experimental results have demonstrated its effectiveness by providing necessary support, and thus reducing user's loading during task execution. The developed system is deemed to be suitable for users with upper limb weakness who can still generate detectable EMG signals. However, practically applying the system to help users achieve effective rehabilitation remains as a challenge. In future work, we aim to enhance system's capability and test it for applications in hospitals.

References

[1] H. Krebs, N. Hogan, M. Aisen, and B. Volpe, "Robot-aided neurorehabilitation," *IEEE transactions on rehabilitation engineering*, vol. 6, no. 1, pp. 75-87, 1998.

[2] P. N. Kooren, J. Lobo-Prat, A. Q. L. Keemink, M. M. Janssen, A. H. A. Stienen, I. J. M. de Groot, M. I. Paalman, R. Verdaasdonk, and B. F. J. M. Koopman, "Design and control of the active A-gear: A wearable 5 DOF arm exoskeleton for adults with duchenne muscular dystrophy," *IEEE Int. Conf. Biomed. Robot. Biomechatronics*, 2016.

[3] S. H. Chen, W. M. Lien, W. W. Wang, G. D. Lee, L. C. Hsu, K. W. Lee, S. Y. Lin, C. H. Lin, L. C. Fu, J. S. Lai, J. J. Luh, and W. S. Chen, "Assistive control system for upper limb rehabilitation robot," *IEEE Transactions on Neural Systems and Rehabilitation Engineering*, vol. 24, no. 11, pp. 1199-1209, 2016.

[4] X. Cui, W. Chen, X. Jin, and S. K. Agrawal, "Design of a 7-dof cable-driven arm exoskeleton (CAREX-7) and a controller for dexterous motion training or assistance," *IEEE/ASME Transactions on Mechatronics*, vol. 22, no. 1, pp. 161-172, 2017.

[5] A. Zeiaee, R. S. Zarrin, A. Eib, R. Langari, and R. Tafreshi, "CLEVERarm: a lightweight and compact exoskeleton for upper-limb rehabilitation," *IEEE Robotics and Automation Letters*, vol. 7, no. 2, pp. 1880-1887, 2022.

[6] A. Garzo, J. H. Jung, J. Arcas-Ruiz-Ruano, J. C. Perry and T. Keller, "ArmAssist: A Telerehabilitation Solution for Upper-Limb Rehabilitation at Home," *IEEE Robotics & Automation Magazine*, vol. 30, no. 1, pp. 62-71, March 2023.

[7] T. Proietti, V. Crocher, A. Roby-Brami and N. Jarrassé, "Upper-limb robotic exoskeletons for neurorehabilitation: a review on control strategies," *IEEE Reviews in Biomedical Engineering*, vol. 9, pp. 4-14, 2016.

[8] N. Lotti and V. Sanguineti, "Estimation of muscle torques from EMG and kinematics during planar arm movements," *IEEE International Conference on Biomedical Robotics and Biomechatronics*, pp. 948-953, 2018.

[9] T. Lenzi, S. M. M. De Rossi, N. Vitiello and M. C. Carrozza, "Intention-based EMG control for powered exoskeletons," *IEEE Transactions on Biomedical Engineering*, vol. 59, no. 8, pp. 2180-2190, Aug. 2012.

[10] J. Furukawa, T. Noda, T. Teramae, and J. Morimoto, "Human movement modeling to detect biosignal sensor failures for myoelectric assistive robot control," *IEEE Transactions on Robotics*, vol. 33, no. 4, pp. 846-857, 2017.

[11] Y. Koike, M. Kawato, "Estimation of dynamic joint torques and trajectory formation from surface electromyography signals using a neural network model," *Biological Cybernetics*, vol. 73, no. 4, pp. 291-300, 1995.

[12] K. Kiguchi and Y. Hayashi, "An EMG-based control for an upper-limb power-assist exoskeleton robot," *IEEE Transactions on Systems, Man, and Cybernetics, Part B: Cybernetics*, vol. 42, no. 4, pp. 1064-1071, 2012.

[13] H. Liang, C. Zhu, Y. Iwata, S. Maedono, M. Mochida, H. Yu, Y. Yan, and F. Duan, "Motion estimation for the control of upper limb wearable exoskeleton robot with electroencephalography signals," *IEEE International Conference on Cyborg and Bionic Systems*, pp. 228-233, 2018.

[14] J. Huang, W. Huo, W. Xu, S. Mohammed, and Y. Amirat, "Control of upper-limb power-assist exoskeleton using a human-robot interface based on motion intention recognition," *IEEE Transactions on Automation Science and Engineering*, vol. 12, no. 4, pp. 1257-1270, 2015.

[15] J.-S. R. Jang, "ANFIS: adaptive-network-based fuzzy inference system," *IEEE Transactions on Systems, Man, and Cybernetics*, vol. 23, pp. 665-685, 1993.

[16] C. H. Ko, S. L. Cheng, K. Y. Young, J. B. Huang, I. Y. Lin, and S. Y. Young, "Design and control of an upper-limb exoskeleton robot with visual sensing," *iRobotics*, vol. 3, no. 1, pp. 10-17, 2020.

[17] S. M. Khan, A. A. Khan and O. Farooq, "Selection of Features and Classifiers for EMG-EEG-Based Upper Limb Assistive Devices—A Review," *IEEE Reviews in Biomedical Engineering*, vol. 13, pp. 248-260, 2020.

[18] Y. Hirata, A. Hara, and K. Kosuge, "Motion control of passive intelligent walker using servo brakes," *IEEE Transactions on Robotics*, vol. 23, no. 5, pp. 981-990, 2007